THE JOURNAL OF PHYSICAL CHEMISTRY B

ARTICLE

pubs.acs.org/JPCB

Polarity Inversion of ζ-Potential in Concentrated Colloidal Dispersions

Héctor M. Manzanilla-Granados, Felipe Jiménez-Ángeles, and Marcelo Lozada-Cassou*

Programa de Ingeniera Molecular, Instituto Mexicano del Petróleo, Lázaro Cárdenas 152, 07730 México, D. F., México

ABSTRACT:

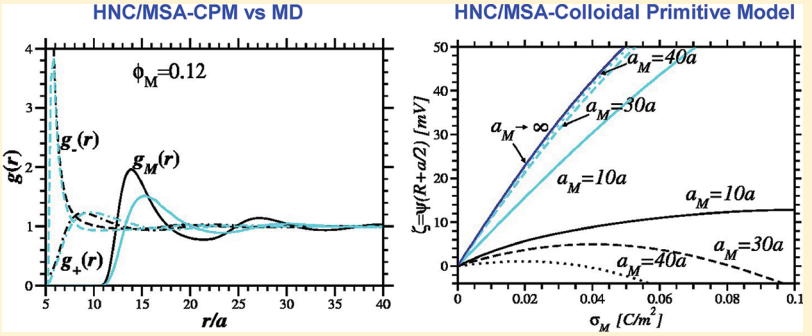

A concentrated colloidal dispersion is studied by applying an integral equations theory to the colloidal primitive model fluid. Important effects, attributed to large size and charge and to the finite concentration of colloidal particles, are found. We observe a polarity inversion of ζ-potential for concentrated colloidal dispersions, while it is not present for a single colloidal particle at infinite dilution. An excellent qualitative agreement between our theoretical predictions and our computer simulations is observed.

The electrical double layer (EDL) refers to the diffuse distribution of charge around a colloidal particle, which is formed when it is placed in contact with a solvent. Many important properties of colloidal dispersions, such as their phase stability, are determined by the electrical double layer. In the case of a single colloidal particle in an electrolyte solution, the EDL has been extensively studied from the beginning of the past century.[1−3] The typical models for the EDL consider a single colloidal particle of certain geometry (spherical, cylindrical, or planar) immersed in an electrolyte solution. The methods developed to study the EDL range from those based on Poisson−Boltzmann equation, density functional and integral equation theories, to sophisticated computer simulation techniques.[4,5] In our group, we have studied the EDL by means of integral equations theory and computer simulations for the planar, cylindrical, and spherical geometries.[5] More recently, we have studied the spherical EDL for several electrolyte models.[6,7]

On the other hand, the interesting case of charged concentrated colloidal dispersions has been considered just in a limited number of cases.[8−13] Theoretical modeling of concentrated colloidal dispersions is of current interest due to the development of a broad diversity of novel synthetic nanoparticles, which acquire charge in solution.[14,15] Recently, we considered a concentrated macroion solution by applying the hypernetted chain/mean spherical approximation (HNC/MSA) to the colloidal primitive model (CPM) fluid,[13] where we compared CPM to the widely used cell model and found qualitative important differences. Here, we extend our CPM integral equation study to include larger macroions and a comparison with our molecular dynamics (MD) simulations. We focus on the radial distribution functions, integrated charge, and mean electrostatic potential profiles, as well as on the ζ-potential for a colloidal particle within a concentrated dispersion. An excellent qualitative agreement between our theoretical predictions and simulation results is observed.

The colloidal primitive model (CPM) consists of a macroion species, plus their counterions and an added electrolyte. All of the fluid components are considered as hard spheres of diameter a_i, at concentration ρ_i, bearing a centered point charge $q_i = z_i e$, with $i = +,-,$M, for the cations, anions, and the macroions, also referred to as the colloidal species, with e being the proton's charge, and z_i the valence for the ith species, with the particularity that $a_+ = a_- = a$ and $a_M \gg a$. The solvent in which these species are immersed is considered as a uniform medium of dielectric coefficient ε_r. The interaction potential between two particles of species i and j, with a separation distance r, is split as $u_{ij}(r) = u^*_{ij}(r) + u^{el}_{ij}(r)$, with the excluded volume interaction preventing two particles from occupying the same position in space, $u^*_{ij}(r) = \infty$ for $r \le a_{ij}$ and 0 for $r > a_{ij}$, where $a_{ij} = (a_i + a_j)/2$. The direct electrostatic interaction is given by the long-range Coulomb potential, $u^{el}_{ij}(r) = k_B T(z_i z_j \ell_B)/(r)$ with $\ell_B \equiv (e^2)/(\varepsilon_r k_B T)$. By definition, the Bjerrum length ℓ_B is the distance at which two unit charges have an interaction energy of $k_B T$. With $\varepsilon_r = 78.5$ for water at room temperature, one gets $\ell_B \approx 7.14$ Å.

Without lost of generality, we consider the macroions to be positively charged, hence, $\rho_- > \rho_+$ because their counterions must be taken into account. Thus, the added electrolyte concentration is $\rho_s = \rho_+$. Furthermore, the fluid is subject to the

Received: April 7, 2011
Revised: August 15, 2011
Published: September 19, 2011

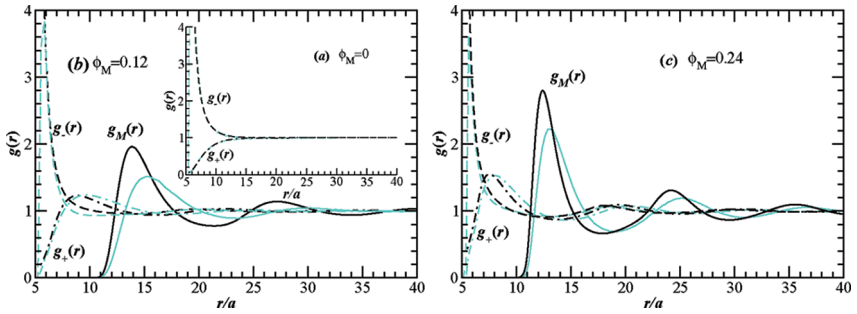

Figure 1. Radial distribution functions (RDFs) for macroions ($g_M(r)$), cations ($g_+(r)$), and anions ($g_-(r)$) around a macroion. Black curves are the results from HNC/MSA-CPM theory, whereas the light-blue curves are the results from MD simulations. The macroions' valence and diameter are z_M = 36, a_M = 10a, respectively, so that σ_M = 0.1C/m^2. The macroions' concentrations are (a) ρ_M = 0, (b) ρ_M = 0.005 M (ϕ_M = 0.12), and (c) ρ_M = 0.01 M (ϕ_M = 0.24). In all cases, ρ_s = 0.1 M and a = 4.25 Å.

electroneutrality condition, that is, $\Sigma_{i=1}^{n} z_i\rho_i = 0$. It is useful to define the macroion surface charge density, $\sigma_M = z_M e/(4\pi R_M^2)$, with $R_M = a_M/2$ being the colloidal radius. The charge around a colloidal particle is compensated by an induced charge, which satisfies $\sigma_M = -(1/4\pi R_M^2)\int \rho_{el}(r)\, dv$, where $\rho_{el}(r)$ is the charge density profile, which is given as $\rho_{el}(r) = \Sigma_{j=+,-,M} q_j\rho_j g_{Mj}(r)$, with $g_{Mj}(r)$ being the radial distribution function (RDF) of the species j around a colloidal particle.

Starting from the n-component Ornstein−Zernike equation, one can straightly derive the hypernetted chain/mean spherical approximation (HNC/MSA) for the CPM,[5] that is:

$$g_{ij}(r) = \exp\{-\beta u_{ij}(r) + \sum_{l=1}^{3} \rho_l \int_v h_{il}(y) c_{lj}^{msa}(s)\, dv_3\} \qquad (1)$$

with i,j = +,−,M, and ρ_l is the number density of species l. $h_{ij}(r) \equiv g_{ij}(r) - 1$, $c_{lj}^{msa}(r)$, and $g_{ij}(r)$ are, respectively, the total, direct, and radial distribution functions for two particles of species i and j. The expressions for the direct correlation function are taken from the analytical mean spherical approximation for a n-component charged fluid.[10,16] Monte Carlo (MC) simulations at zero salt concentration have been performed in the past.[8,9] For validation purposes, we solved our HNC/MSA theory for zero salt concentration and monovalent counterions and found a good agreement with the Linse and Lobaskin MC data.[8] However, we have not included this comparison here.

In molecular simulations, for the excluded volume interaction between the ions, we use the following potential: $u^*_{ij}(r) = 4\varepsilon[((a)/(r - r_s))^{12} - ((a)/(r - r_s))^6 + 1/4]$ for $0 < r \le r_{cut} + r_s$ with $r_{cut} \equiv 2^{1/6}a$ and $u^*_{ij}(r) = 0$ for $r > r_{cut} + r_s$. Setting $r_s = a_{ij} - a$ gives a distance of closest approach of $r_s + a = a_{ij}$. We performed Molecular Dynamics (MD) simulations using the Espresso package.[17] For the simulations, we employed a Langevin thermostat to drive the system into the canonical state. Also, we used an accelerated FFT Ewald sum, that is, the P^3 M algorithm, to deal with electrostatic long-range interactions and periodic boundary conditions. The presented results originate from averaging over roughly 5000 independent configurations.

We have solved eq 1 to obtain the radial distribution functions (RDFs) for cations ($g_{M+}(r)$), anions ($g_{M-}(r)$), and colloids ($g_{MM}(r)$) around a central colloidal particle. Hereinafter, we refer to these functions simply as $g_+(r)$, $g_-(r)$, and $g_M(r)$. The mean electrostatic potential, $\psi(r)$, ζ-potential, $\zeta \equiv \psi(R_M + a/2)$, and the integrated charge density profiles, $\sigma(r)$, are straightly obtained.[13] The colloid concentration in the CPM fluid is expressed in terms of their volume fraction, $\phi_M \equiv \pi\rho_M a_M^3/6$. The Debye length is $\kappa_s^{-1} \equiv (8\pi e^2 z^2 \rho_s/\varepsilon_r)^{-1/2}$, which takes into account only the added salt. We considered that the little ions are always monovalent, are at 0.1 M concentration, and their diameter is a = 4.25 Å. The integrated total charge density profile is defined as

$$\sigma(r) \equiv \sigma_M \frac{R_M^2}{r^2} + \frac{1}{r^2}\int_{RM + a/2}^{r} \rho_{el}(y) y^2\, dy \qquad (2)$$

where the first term at the right-hand side is the central macroion contribution, and the second term is the accumulated charge per unit area between the surface of the central colloidal particle and a spherical shell of radius $r > R_M + a/2$.

First, we analyze the electric double layer (EDL) around a colloidal particle. In Figure 1a, the RDFs from HNC/MSA theory and MD simulations for cations and anions around a single spherical macroparticle, that is, when the colloidal dispersion is at infinite dilution ($\phi_M = 0$), show a monotonic behavior. A quantitative agreement is observed. This behavior is consistent with the classical Poisson−Boltzmann theory.[6] For the concentrated cases, in Figure 1b and c, we show the RDFs for cations, anions, and macroions around a macroion, for ϕ_M = 0.12 and 0.24, respectively. In all cases, the macroions' diameter is a_M = 10a, and their valence is z_M = 36, while the salt concentration is ρ_s = 0.1 M. For the concentrated macroions' dispersions, the RDFs for little ions are not monotonic, as for the infinite dilution case. Instead, the EDL is more compact and the anions adsorption is higher as the macroions' concentration increases: HNC/MSA predicts $\rho_- g_-(R_M + a/2) \approx 2$ and 2.6 M for ϕ_M = 0.12 and ϕ_M = 0.24, respectively, whereas $\rho_- g_-(R_M + a/2) \approx 1.4$ M for ϕ_M = 0. The higher adsorption of anions gives rise to charge reversal,[10] implying that the charge of the central colloid is overcompensated by the adsorbed anions, originating from the adsorption of cations in a second layer, which is seen as a maximum of their RDF. The macroions' RDF shows a depletion region where $g_M(r) \approx 0$ at the neighborhood of the central colloidal particle, followed by a maximum to end up in damped oscillations around 1. The distance to the location of such a maximum from the center of the macroion, referred to as the correlation length l_C, decreases as ϕ_M and/or σ_M increase. For the two cases shown in Figure 1, our integral equations theory predicts a correlation length of $l_C \approx 14a$ and 12.5a for ϕ_M = 0.12 and 0.24, respectively, while MD simulations give $l_C \approx 15a$ and 13a for the same concentrations.

It should be pointed out the quantitative agreement between HNC/MSA theory and MD simulations for ϕ_M = 0. For the

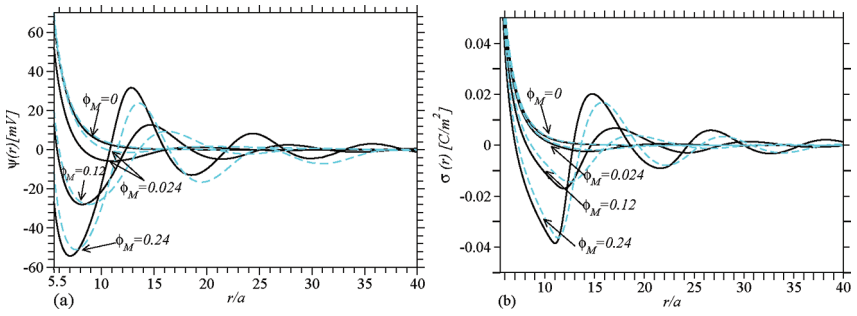

Figure 2. (a) Mean electrostatic potential profiles, $\psi(r)$, and (b) integrated charge density profiles, $\sigma(r)$, around a macroion. Black curves are the results from HNC/MSA-CPM theory, whereas the light-blue curves are the results from MD simulations. The results are for $\rho_M = 0$ M ($\phi_M = 0$), $\rho_M = 0.001$ M ($\phi_M = 0.024$), $\rho_M = 0.005$ M ($\phi_M = 0.12$), and $\rho_M = 0.01$ M ($\phi_M = 0.24$), respectively. The macroions' valence and diameter are $z_M = 36$ and $a_M = 10a$, respectively, so that $\sigma_M = 0.1\text{C/m}^2$. The concentration of the added electrolyte is $\rho_s = 0.1$ M.

concentrated cases, the main discrepancies observed between theory and simulation are at the maximum of the macroion−-macroion RDFs: HNC/MSA theory predicts the location of this maximum shifted to the left and higher with respect to the results from MD simulations. Concerning the macroion−anion RDFs, it is observed that HNC/MSA theory overestimates the contact value at $r = R + a/2$. This is, of course, consistent with the observed differences in l_C, between the HNC/MSA and MD results. Despite these differences between theory and MD simulations, it can be considered that the theory properly captures the physical behavior of the system.

In Figure 2a, we plot the mean electrostatic potential profile, $\psi(r)$, from HNC/MSA and MD simulations, for successive increasing macroions' concentrations. An oscillatory behavior of $\psi(r)$ for the concentrated macroions' dispersions is exhibited here, while for $\phi_M = 0$ it is monotonic. It should be pointed out that for the cell model, $\psi(r)$ is monotonic.[13] The intensity and range of the oscillations increase as the macroions' concentration increases. The contact value of the mean electrostatic potential, $\zeta = \psi(R + a/2)$, decreases as the colloids concentration increases and becomes negative for the most concentrated solution. Charge reversal is manifested as a change of slope of the $\psi(r)$ profile preceded by a local minimum, which indicates an inversion of the local electric field. The magnitude of the electrical field around a colloid is given as $E(r) = -(\partial\psi(r))/(\partial r) = (\sigma(r))/(\varepsilon_r)$. The field inversion is more intense as the colloids concentration increases; meanwhile, it is absent for zero colloids concentration. A similar behavior is observed for successively increasing macroions' charge and by keeping constant the macroions' volume fraction (ϕ_M).

The decreasing, monotonic, behavior of $\psi(r) \geq 0$, as $r \rightarrow \infty$, for macroparticles at infinite dilutions implies a decreasing, monotonic, electrical field $E(r) \geq 0$. However, the connection between $E(r)$ and $\psi(r)$ is not so simple for the concentrated cases presented here. As pointed out above, $E(r) = (\sigma(r))/(\varepsilon_r)$, hence, a better understanding of the charge distribution around a colloidal particle is provided by the integrated charge density, $\sigma(r)$, rather than by only the mean electrostatic potential profile (see eq 2). In Figure 2b, the value of $\sigma(r)$ at $r = R_M = 5a$ is always equal to σ_M, meaning that the accumulated charge at this point is equal to the charge of the colloidal particle. As r increases, $\sigma(r)$ decreases, reflecting the fact that the colloid's charge is compensated by its counterions. When $\sigma(r)$ is below zero, the colloid's charge is overcompensated (charge reversal), whereas the first maximum of this function is due to the adsorption of colloids at a

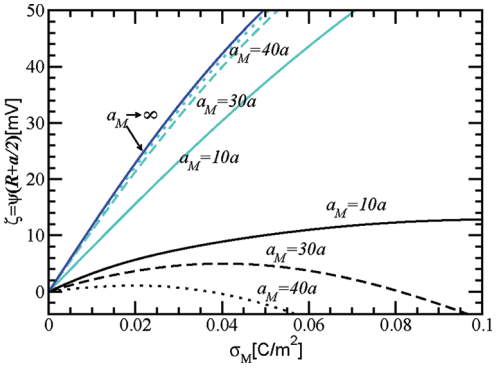

Figure 3. ζ-Potential for a colloidal particle as a function of its surface charge density, σ_M, for three different colloids diameters: $a_M = 10a$ (−), $a_M = 30a$ (− − −), and $a_M = 40a$ (· · ·). Black curves are for a concentrated colloidal dispersion at $\phi_M = 0.12$, whereas the light-blue curves are for a colloidal particle at infinite dilution, that is, $\phi_M = 0$. The dark blue curve is for $a_M \rightarrow \infty$, that is, the semi-infinite planar wall limit. In all cases, $\rho_s = 0.1$ M and $a = 4.25$ Å.

second layer next to the charge reversal layer. Charge reversal by counterions and the macroions' adsorption at the contiguous layer is more important as their concentration increases. The following damped oscillatory behavior of $\sigma(r)$ is a consequence of the alternating layers of little ions and macroions. For the zero colloids concentration, $\sigma(r)$ decreases monotonically from σ_M to 0; meanwhile, charge reversal for the most concentrated case is very high. It should be pointed out that the inversion of the polarity of ζ-potential does not imply an inversion of the colloid's electrical field at the slipping plane, that is, $r = R_M + a/2$, as can be clearly seen from Figure 2a and b.

If the macroions' charge is considered to be uniformly distributed on their surface, by Gauss's law eq 1 does not change, which implies that the radial distribution functions do not change for this new model. However, because now the charge distribution is on the macroparticles surface, a new integrated charge density profile, as defined by eq 2, will be found and will be different from those in Figure 2b. This new charge density profile implies a new electrical field and mean electrostatic potential profile. We will explore this approach in a forthcoming publication. Here, we advance that for this model the charge reversal and other properties will change. In general, they will be less pronounced. One can consider other charge distributions of the macroions' charge, and in every case different integrated

charge density and mean electrostatic potential distributions will be obtained.

In colloid science, the ζ-potential is the mean electrostatic potential in the interfacial double layer at the location of the slipping plane of a colloidal particle.[18] The ζ-potential can be related to the electrophoretic mobility of a colloidal particle, μ_E, which is an observable typically used to estimate the colloidal effective charge.[19−21] In Figure 3 are presented the results for the ζ-potential as a function of σ_M from HNC/MSA for three different colloidal diameters, that is, a_M = 10a, 30a, and 40a. The colloids volume fraction is kept constant at ϕ_M = 0.12, and the added electrolyte concentration is always ρ_s = 0.1 M. For reference, we included the infinite dilution cases (ϕ_M = 0) for the same colloidal diameters and electrolyte concentration. Typically, for a single macroparticle at infinite dilution, ζ increases monotonically with σ_M and is higher as its diameter increases. This is also the case for the cell model.[13] Approximately for $a_M \gtrsim 40a$, ζ reaches a limiting value; that is, it corresponds to a semi-infinite charged planar wall. For the concentrated cases, the ζ-potential exhibits a nonmonotonic behavior as a function of σ_M: It increases for low values of σ_M, reaches a maximum, starts decreasing, and becomes negative above a certain value of σ_M. For a fixed surface charge density, there is a clear tendency of ζ to decrease as the colloid diameter increases in opposition to the infinite dilution case. Moreover, we observed that ζ may approach the limiting curve for $a_M \rightarrow \infty$ only for $\phi_M \rightarrow 0$. As soon as either ϕ_M or σ_M becomes relevant, the value of ζ deviates from such a limiting value.

From a fundamental point of view, the optimization of the accessible volume is the underlying mechanism behind charge reversal and the polarity inversion of ζ-potential. That is, by adsorbing more counterions toward a macroparticle surface than the necessary to compensate its bare charge, the system releases space and, hence, maximizes entropy.[10] The macroions' excluded volume is composed of two contributions: the particles' volume fraction itself, ϕ_M, and the excluded volume produced by their mutual electrostatic repulsion, which intuitively can be quantified by the parameter $\xi = (z_M{}^2e^2)/(k_BTa_M) = (\pi^2a_M{}^3\sigma_M{}^2)/(k_BT)$.[10] It can be seen from here that the electrostatic excluded volume increases with the macroparticle's diameter even if their surface charge density and volume fraction are kept constant. Hence, the polarity inversion of ζ-potential and charge reversal are expected whenever the macroions' excluded volume is high, as can be seen in Figure 3. A nonmonotonic behavior of the ζ versus σ_M curve, with a maximum for some values of σ_M, and the decreasing tendency of ζ, as a_M increases, in opposition with the ϕ_M = 0 case, resembles clearly the ζ versus σ_M curve found for the spherical EDL, where only the electrolyte is present, as a result of increasing the electrolyte concentration or valence.[6] Figure 3 will be different for different charge distributions of the macroions' charge, for example, if the charge is uniformly distributed on the macroions' surface.

In summary, the electric double layer for a particle in a concentrated colloidal dispersion has been studied by means of the well-established hypernetted chain/mean spherical approximation and by means of molecular dynamics simulations. When the colloidal particles are sufficiently charged and/or concentrated, the polarity of their ζ-potential is reversed. Such an inversion is always associated with the colloidal surface charge reversal. This behavior is not observed for the same colloidal particles at infinite dilution. The theoretical predictions are in excellent qualitative agreement with the results from molecular dynamics, for the cases where computer simulations are accessible. We find it interesting that the general qualitative behavior of ζ versus σ_M resembles closely that of the simple electrolyte spherical EDL.[6] We wish to highlight that we have developed a theoretical approach capable of accounting for concentrated dispersions made up of charged macroparticles of colloidal dimensions.

AUTHOR INFORMATION

Corresponding Author

*E-mail: marcelo@imp.mx.

ACKNOWLEDGMENT

F.J.-A. thanks Prof. Christian Holm for his hospitality during a simulation workshop at Institut für Computerphysik, Universität Stuttgart. F.J.-A. also thanks Centre Europén de Calcul Atomique et Moléculaire for supporting part of his stay at Universität Stuttgart.

REFERENCES

(1) Gouy, G. *J. Phys. (Paris)* **1910**, *4*, 457.
(2) Chapman, D. L. *Philos. Mag.* **1913**, *25*, 475.
(3) Lyklema, J. *Fundamentals of Interface and Colloid Science, Fundamentals*; Academic Press: New York, 1991; Vol. I.
(4) Attard, P. *Curr. Opin. Colloid Interface Sci.* **2001**, *6*, 366.
(5) Lozada-Cassou, M. In *Foundamental of Inhomogeneous Fluids*; Henderson, D., Ed.; Marcel Dekker: New York, 1993; Chapter 8.
(6) González-Tovar, E.; Lozada-Cassou, M. *J. Phys. Chem.* **1989**, *93*, 3761.
(7) Degrève, L.; Lozada-Cassou, M.; Sánchez, E.; González-Tovar, E. *J. Chem. Phys.* **1993**, *98*, 8905. Guerrero-García, G. I.; González-Tovar, E.; Lozada-Cassou, M.; Guevara-Rodríguez, F. de J. *J. Chem. Phys.* **2005**, *123*, 034703. González-Tovar, E.; Jiménez-Ángeles, F.; Messina, R.; Lozada-Cassou, M. *J. Chem. Phys.* **2004**, *120*, 9782. Guerrero-García, I.; González-Tovar, E.; Chávez-Páez, M.; Lozada-Cassou, M. *J. Chem. Phys.* **2010**, *132*, 054903.
(8) Linse, P.; Lobaskin, V. *Phys. Rev. Lett.* **1999**, *83*, 4208. *J. Chem. Phys.* **1999**, *111*, 4300.
(9) Hribar, B.; Vlachy, V. *Biophys. J.* **2000**, *78*, 694.
(10) Jiménez-Ángeles, F.; Lozada-Cassou, M. *J. Phys. Chem. B* **2004**, *108*, 7286. **2004**, *108*, 1719.
(11) Takamichi, T.; Tsuneyoshi, N. *Phys. Rev. E* **2002**, *65*, 021405.
(12) Jiménez-Ángeles, F.; Odriozola, G.; Lozada-Cassou, M. *J. Phys.: Condens. Matter* **2009**, *21*, 424107.
(13) Manzanilla-Granados, H. M.; Jiménez-Ángeles, F.; Lozada-Cassou, M. *Colloids Surf., A* **2011**, *376*, 59.
(14) Tohver, V.; Smay, J. E.; Braem, A.; Braun, P. V.; Lewis, J. A. *Proc. Natl. Acad. Sci. U.S.A.* **2001**, *98*, 8950.
(15) Mishra, P. P.; Pigga, J.; Lu, T. *J. Am. Chem. Soc.* **2008**, *130*, 1548.
(16) Blum, L. *Mol. Phys.* **1975**, *30*, 1529.
(17) Limbach, H.-J.; Arnold, A.; Mann, B. A.; Holm, C. *Comput. Phys. Commun.* **2006**, *174*, 704.
(18) Delgado, A. V.; González-Caballero, F.; Hunter, R. J.; Koopal, L. K.; Lyklema, J. *J. Colloid Interface Sci.* **2007**, *309*, 194.
(19) OBrien, R. W.; White, L. R. *J. Chem. Soc., Faraday Trans. 2* **1978**, *74*, 1607.
(20) Ohshima, H. *Colloids Surf., A* **2005**, *267*, 50.
(21) Lozada-Cassou, M.; González-Tovar, E. *J. Colloid Interface Sci.* **2001**, *239*, 285. Lozada-Cassou, M.; González-Tovar, E.; Olivares, W. *Phys. Rev. E* **1999**, *60*, R17.